Journal of the Physical Society of Japan
Vol. 75, No. 1, January, 2006, 014201

Decay of ^{101}Mo and Band Structures of its Daughter Nuclide ^{101}Tc in the Projected Shell Model

Shen SHUIFA[1,2,3*], Wang FENGGE[4], Gu JIAHUI[5], Liu YUJUAN[1], Tang BIN[1] and Jiang WEIZHOU[5]

[1]*School of Nuclear Engineering and Technology, East China Institute of Technology, Fuzhou 344000, Jiangxi, People's Republic of China*
[2]*School of Physics, Peking University, Beijing 100871, People's Republic of China*
[3]*CCAST (World Laboratory), P. O. Box 8730, Beijing 100080, People's Republic of China*
[4]*School of Electric and Information Engineering, Zhongyuan University of Technology, Zhengzhou 450007, Henan, People's Republic of China*
[5]*Shanghai Institute of Applied Physics, The Chinese Academy of Sciences, Shanghai 201800, People's Republic of China*

(Received July 23, 2005; accepted November 9, 2005; published January 10, 2006)

The decay of molybdenum-101 has been investigated using the three-parameter (γ–γ–t) coincidence system of HPGe–HPGe detectors. According to the off-line analysis, the decay scheme was modified. The positions of 221.80, 318.00, 377.90, 452.50, 515.42, 1011.05, and 1759.72 keV transitions have been arranged again, the transition positions of 104.70, 105.95, and 774.15 keV gamma rays have been assigned for the first time, the positions of 169.00, 590.91, 980.52, and 1431.68 keV transitions have been reconfirmed, and the 1508.01 keV gamma ray was observed simultaneously for the first time and its transition position has been assigned. The β^- intensities and the values of log *ft* of most levels were calculated. Combining with the high-spin states observed by the in-beam γ-ray spectroscopy of previous decay works, the structure of the excited positive/negative-parity yrast states of ^{101}Tc is discussed using a projected shell model, and a band diagram calculated for the positive-parity yrast band is also shown in order to extract physics out of the numerical results. In addition, the analysis of other three bands originated from $3/2^-[301]$, $5/2^-[303]$, and $1/2^+[431]$ Nilsson states, respectively, is also performed in the framework of this model.

KEYWORDS: decay, γ-ray, level, coincidence, PSM, yrast states
DOI: 10.1143/JPSJ.75.014201

1. Introduction

The neutron-rich transitional nuclei in the $A \sim 100$ mass region display complex structures which are amenable to neither shell-model calculations nor to geometrical model approaches,[1)] and they have been studied extensively in recent years.[2)] One of the main reasons is the nature of the shape transition, which display a complex low-lying structure. The coexistence and competition between various forces acting inside these nuclei is responsible for this complex structure. The existence of two subshell closures, $Z = 38$ or 40 and $N = 56$, as well as the disappearance of these energy gaps for specific nucleonic numbers contribute to the complexity of the low-lying structures. In particular, transitional nuclei with numbers of active nucleons intermediate between the two limits, spherical and strongly deformed, are more difficult to describe. The present work reports on level structures in the odd-Z $^{101}_{43}Tc_{58}$ nucleus which had been already investigated by some groups.[1–3)]

On the other hand, let us have an examination of low-energy and low-spin part of the ^{101}Tc level scheme. Detailed information on states with low-spin values and low excitation energies can be obtained using γ-ray (and conversion electron) spectroscopy following radioactive decay. The β^- decay of ^{101}Mo ($T_{1/2} = 14.61$ min) presents an excellent way to get information about the low energy levels of ^{101}Tc. A present decay scheme of ^{101}Mo was built mainly according to the single spectra measurement by Hammed *et al.*[4)] in 1993 and the γ–γ coincidences measurement by Wright *et al.*[5)] in 1975. It should be pointed out that many γ-rays which belong to the decay of ^{101}Mo were not placed in level scheme.[4–6)] The nuclear structure of ^{101}Tc which is daughter of ^{101}Mo was studied using the ^{100}Mo(^{3}He, pnγ) reaction in 1997 by Savage *et al.*,[3)] the experiments included γ-ray excitation functions, γ-ray angular distributions, and γ–γ coincidences measurement. The results were interpreted using a particle-rotor model. Careful analyzing of the decay scheme of ^{101}Mo proposed by Hammed *et al.*[4)] and the level scheme for ^{101}Tc proposed by Savage *et al.*,[3)] it can be found that there are some discrepancies. For example, the 515.42 keV γ-ray is placed between the level at 1122.04 keV and the level at 606.46 keV in ref. 4, meanwhile the 515.1 keV γ-ray is placed between the level at 515.16 keV and the ground state in ref. 3. These discrepancies have motivated us to use the coincidence technique of HpGe detectors to reexamine ^{101}Mo decay.

In this work the results of our investigation of the ^{101}Tc isotope in radioactive decay is presented. Preliminary results of this work have been published elsewhere.[7)] In §2 the experimental procedures are presented. Section 3 reports on the model independent decay scheme construction, and in §4 the interpretation of the level scheme in the framework of the projected shell model (PSM) is presented.

2. Experimental Procedures

The radioactive sources of ^{101}Mo were produced by neutron irradiation of 1 mg targets of metallic ^{100}Mo isotopically enriched to 99.2% via the reaction ^{100}Mo(n,

*E-mail: shfshen@ecit.edu.cn

Table I. New γ–γ coincidence relationships observed in the decay of ^{101}Mo.

Gate (keV)	Coincident γ-rays (keV)	Placement (keV)
80.92	105.95, 318.00	394.77–288.45, 606.46–288.45
195.93	515.42	515.250–0.0
211.98	169.0	669.80–500.43
221.80	80.92, 105.95, 378.99, 571.62	288.45–207.517, 394.77–288.45, 394.77–15.602, 1188.04–616.20
333.61	1508.01	2129.83–622.06
408.69	774.15, 1431.68	1962.326–1188.04, 2047.72–616.20
510.21 + 512.83 + 514.1 + 515.42	195.93	711.205–515.250
566.62	452.5	2047.72–1594.65
590.10 + 590.91	104.70	711.205–606.46
606.8 + 608.34	104.70	711.205–606.46
642.71	590.91	606.46–15.602
774.15 + 775.8	980.52	1188.04–207.517
869.7 + 871.08	1011.05	1897.97–886.70
877.39	1011.05	1897.97–886.70
980.52	774.15	1962.326–1188.04
1011.05 + 1012.47	871.08, 877.39	886.70–15.602, 886.70–9.320
1249.4 + 1251.10	104.70	711.205–606.46
1346.09	221.80	616.20–394.77
1530.3 + 1532.49	515.42	515.250–0.0
1662.49	377.9	2056.83–1678.09
1754.90 + 1759.72	80.92	288.45–207.517

γ)^{101}Mo. The neutron beam, whose energy was ~6 MeV, was produced from irradiation of ^{9}Be using 16 MeV, 5 μA deuterium,[8] which was produced from the $K = 40$ Cyclotron in Shanghai Institute of Applied Physics and passed through the Havar film of 20 μm thick. The only detectable contaminants in the sources were ^{99}Mo ($T_{1/2} = 2.75$ d) and ^{97}Zr($T_{1/2} = 16.9$ h), which were formed from the reactions ^{100}Mo(n, 2n)^{99}Mo and ^{100}Mo(n, α)^{97}Zr, respectively. Due to the difference in half-life, a short-term irradiation of ^{100}Mo can be used to produce sufficient interference-free activity for the determination of the decay of ^{101}Mo. There can also be found some γ-rays from the decay of ^{101}Tc, the daughter of ^{101}Mo.

A series of coincidence measurements were carried out in order to establish the relationship among the γ-rays observed. The experiments were performed with the three-parameter γ–γ–t data acquisition system composed of two hyper-pure Ge γ-ray detectors. One of the detectors was a planar Ge detector (GMX-20190) with 20% efficiency and 1.85 keV resolution at 1332 keV, the other was a coaxial Ge detector (GEM-50195) with 50% efficiency and 2.0 keV resolution at 1332 keV. The experiments are carried out for 20 times, the irradiation time and measurement time is selected 30 and 45 min, respectively. A total of 1×10^7 coincidence events were written on an event-by-event basis on magnetic tapes for off-line analysis. Figure 1 shows the coincidence γ-ray spectra gated on several photopeaks. Table I lists the new coincidence relationships observed.

In addition, according to the in-beam gamma experimental results given by Savage *et al.*,[3] the spin and parity of $5/2^-$, $5/2^+$, $7/2^+$, $3/2^-$, $1/2^-$ or $3/2^-$, $3/2^-(5/2^-)$, $3/2^+$ or $5/2^+$, $3/2^-$ or $5/2^-$, and $3/2^+$ or $5/2^+$ were assigned to the 500.43-, 515.250-, 533.55-, 616.20-, 622.06-, 669.80-, 711.205-, 1188.04-, and 1319.57-keV levels, respectively.

3. Decay Scheme

The decay scheme of ^{101}Mo deduced from the present work is shown in Fig. 2. Absolute γ-ray emission probabilities (P_γ) were derived from the evaluated relative emission probability by requiring that the sum of all transitions (γ-rays plus conversion electrons) to either the ground state and the first two excited states of ^{101}Tc from higher levels should be equal to 1 (100%). The intensities of the conversion electrons were used just as Hammed *et al.* adopted in their work.[4] This method avoids the need to include information about the 6.3 and 15.6 keV transitions of ^{101}Mo which are highly internally converted. It was also assumed that there is no direct beta decay to these levels, an assumption justified by these three spin-parity assignments. The relative intensities with their uncertainties and energies of all γ-rays in the decay scheme were taken from ref. 4, except for the energy of 1508.01 keV γ-ray, which is deduced from our present work, and its relative intensity is not given because it could not be resolved in the singles spectra. Now that we now assign that the 515.45 keV γ-ray is the transition from the level at 515.05 keV to the ground state, and the 1759.72 keV γ-ray is the transition from the level at 2047.72 keV to the level at 288.45 keV, normalized according to ref. 4, the absolute intensity of every γ-ray should be revised, they should multiply by the factor 1.00826(100/99.181).

The intensities of the beta branches feeding to the ^{101}Tc were determined from the transition deficits (transition intensity from a level minus the intensity to that level). The internal conversion electrons and all possible γ-rays to and from levels are carefully included in the uncertainties for the β^- branches for the relevant levels. We calculated the β^- decay branching over again due to the change of some γ-

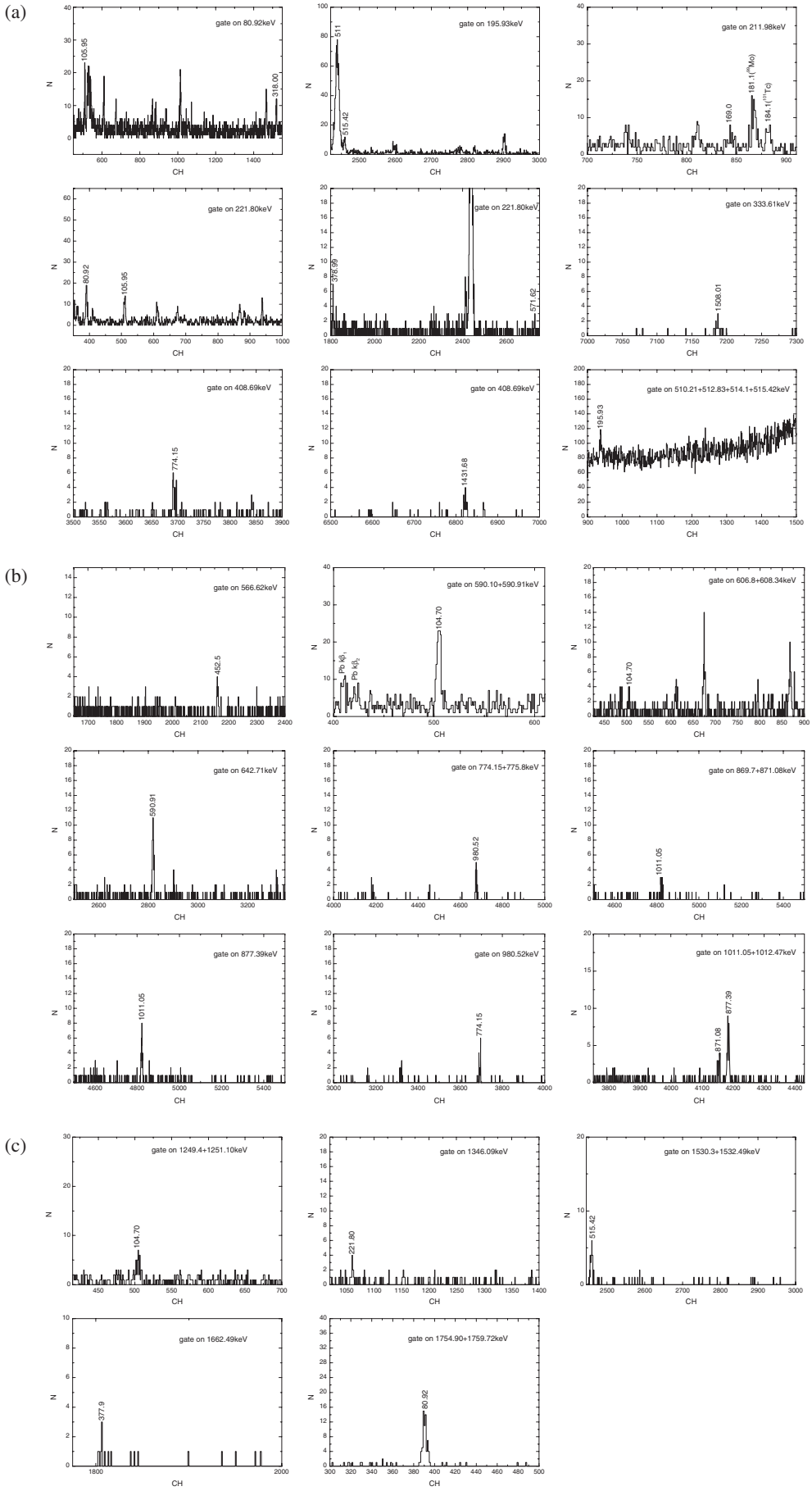

Fig. 1. Coincidence spectra obtained by gating on several peaks, which establish new γ–γ coincidence relationships. The numbers near peaks are γ-ray energies in keV.

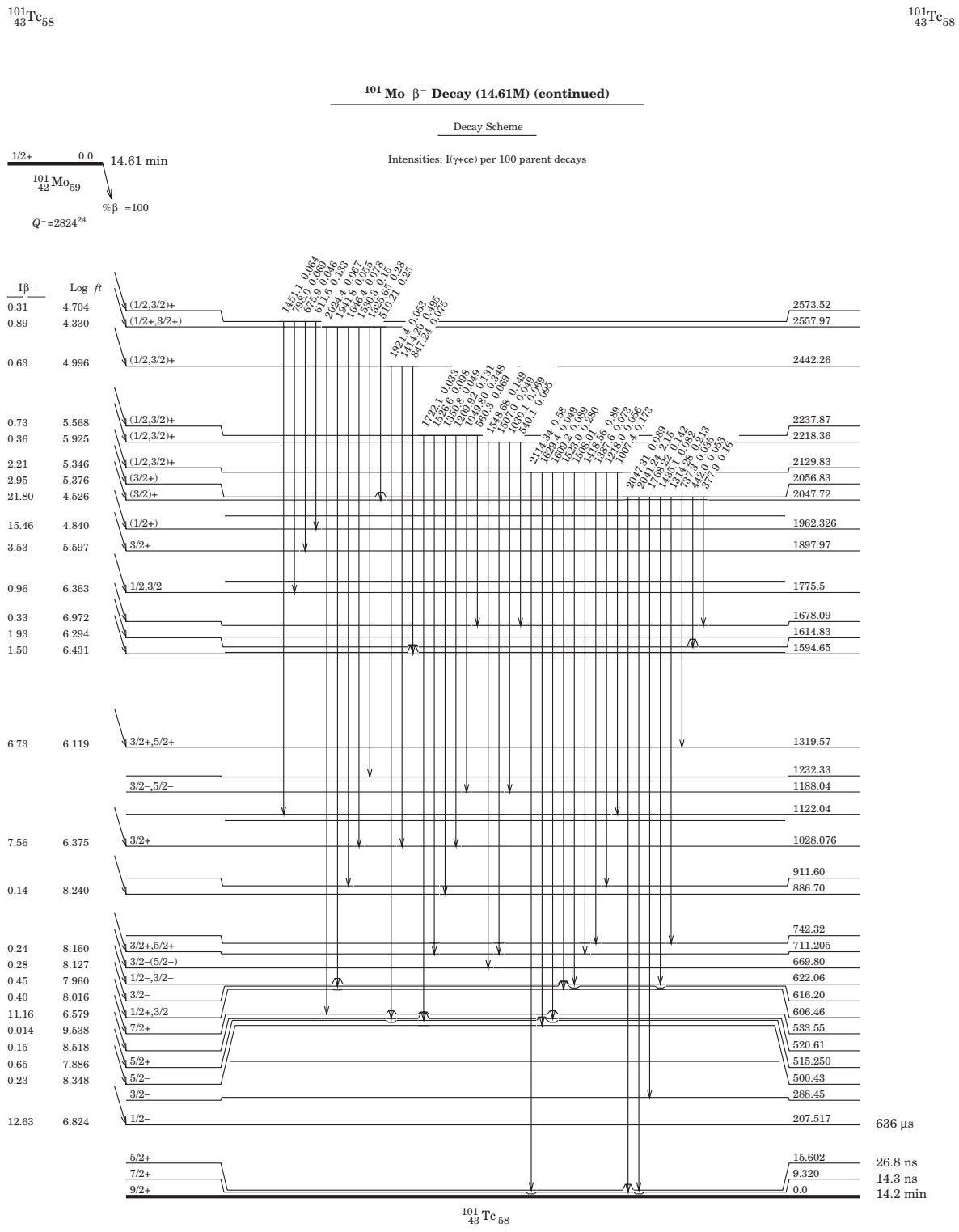

Fig. 2. The proposed decay scheme of ^{101}Mo established in this experiment.

rays, but the 1508.01 keV γ-ray was not taken into account.

The log *ft* values for the β^- branches to the ^{101}Tc levels were calculated by using the Evaluated Nuclear Structure Data File (ENSDF) analysis and checking program offered by the National Nuclear Data Center (NNDC) at Brookhaven National Laboratory. The result is presented in the decay scheme (Fig. 2), and in the Table II the standard uncertainty in log *ft* values are given.

4. Calculations in the Framework of the Projected Shell Model

This paper reports our investigation of total five bands identified in ^{101}Tc. The structure of the positive/negative-parity yrast states in ^{101}Tc were already discussed extensively in the previous studies. The former has a $\pi g_{9/2}$ configuration, whereas the latter is interpreted as arising from a $\pi p_{1/2}$ configuration mixed with other negative parity

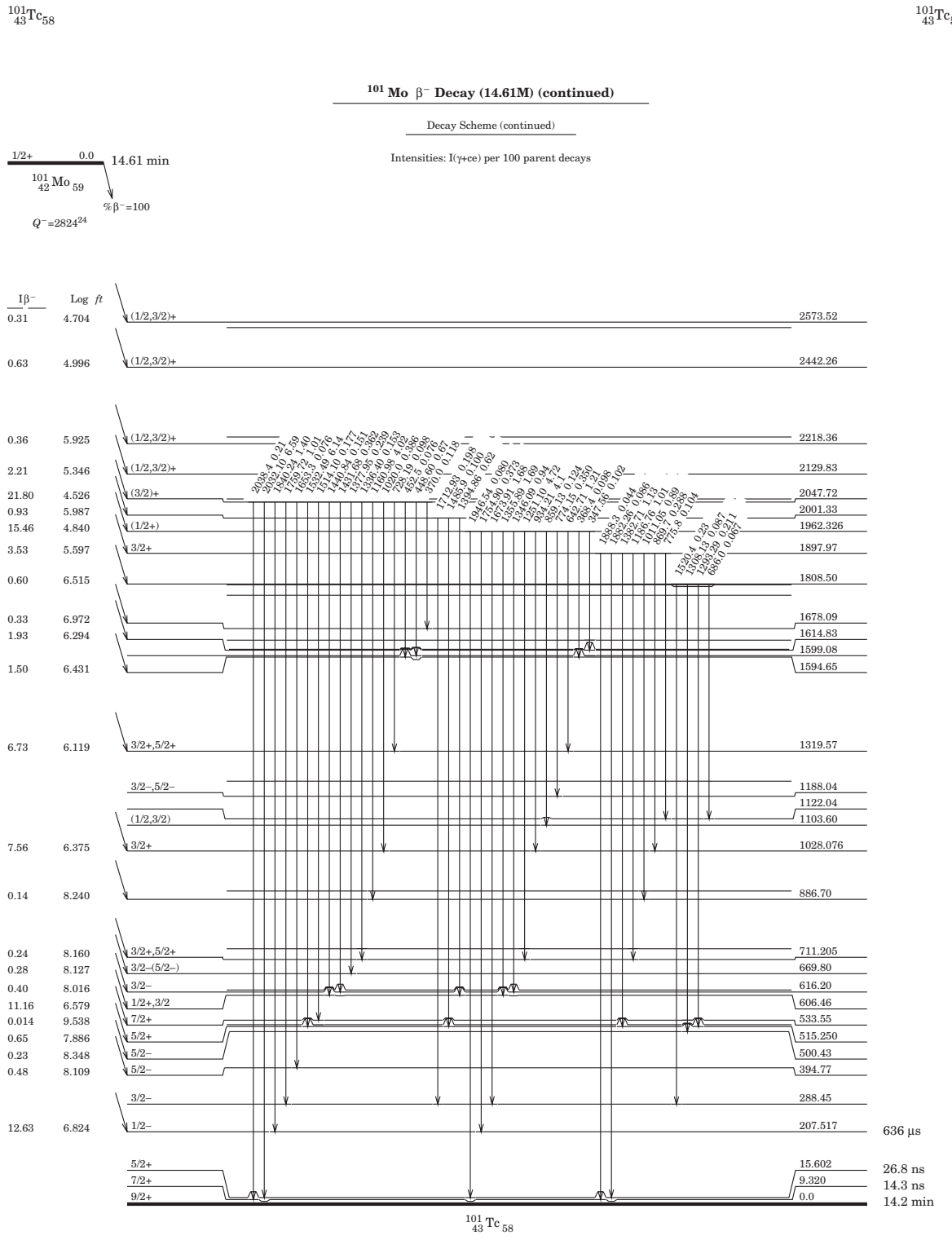

Fig. 2. *continued*

orbitals in an asymmetric rotor description.[1)] In this work, we used this PSM to study neutron-rich nuclei in the mass-100 region. A detailed description of the PSM is given in ref. 9, and in the present work we stress the calculations and discussion aimed at the elucidation of the nucleus ^{101}Tc. In recent years, this theoretical model has become quite successful in describing a broad range of properties of deformed nuclei in various regions of the nuclear Periodic Table. The most striking aspect of this quantum mechanical model is its ability to describe the finer details of the high-spin spectroscopy data with simple physical interpretations.[10)] In this work, we try to apply this model to the mass region around $A = 100$ and to show the potential of this model via the study of low- and high-spin states of this transitional nucleus.

In these PSM calculations the values of the Nilsson parameters of the modified oscillator potential, κ and μ, correspond to the values given in ref. 11. The pairing

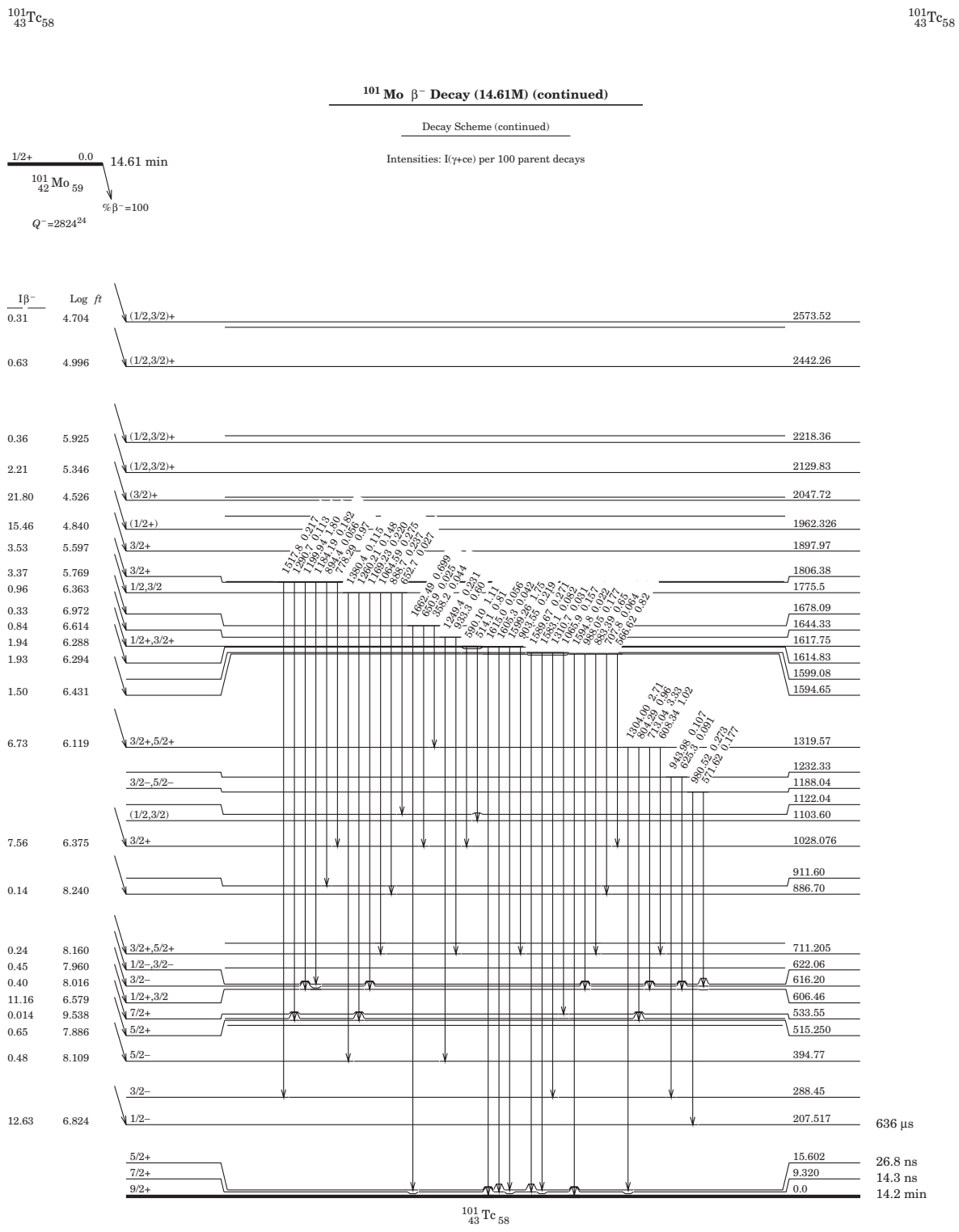

Fig. 2. *continued*

strength Δ was deduced from the odd even mass differences.[12] The values of the total nuclear binding energy B are taken from ref. 13, and the experimental data are adopted if only they can be supplied. The results are $\Delta_p = 1.5725$ MeV and $\Delta_n = 0.9275$ MeV. Pairing is treated by the BCS formalism. In the pairing correlations we included three oscillator shells, $N = 3, 4, 5$ for the neutrons and $N = 2, 3, 4$ for the protons. Shape calculations using the Nilsson + BCS formalism were carried out for the nucleus ^{101}Tc, the Hartree–Fock–Bogoliubov energy E_{HFB} (approximately equivalent to the deformation energy from the calculations using the Nilsson + BCS method[14]) of ^{101}Tc as a function of quadrupole deformation ε_2 is shown in Fig. 3. It can be found that the energy E_{HFB} has two minima in Fig. 3, they correspond to the prolate shape ($\varepsilon_2 = 0.28$) and the spherical shape ($\varepsilon_2 = 0.00$), respectively, and that these two minima are considered the possible forms of equilibrium deformation. From the previous works, it is indicated that this

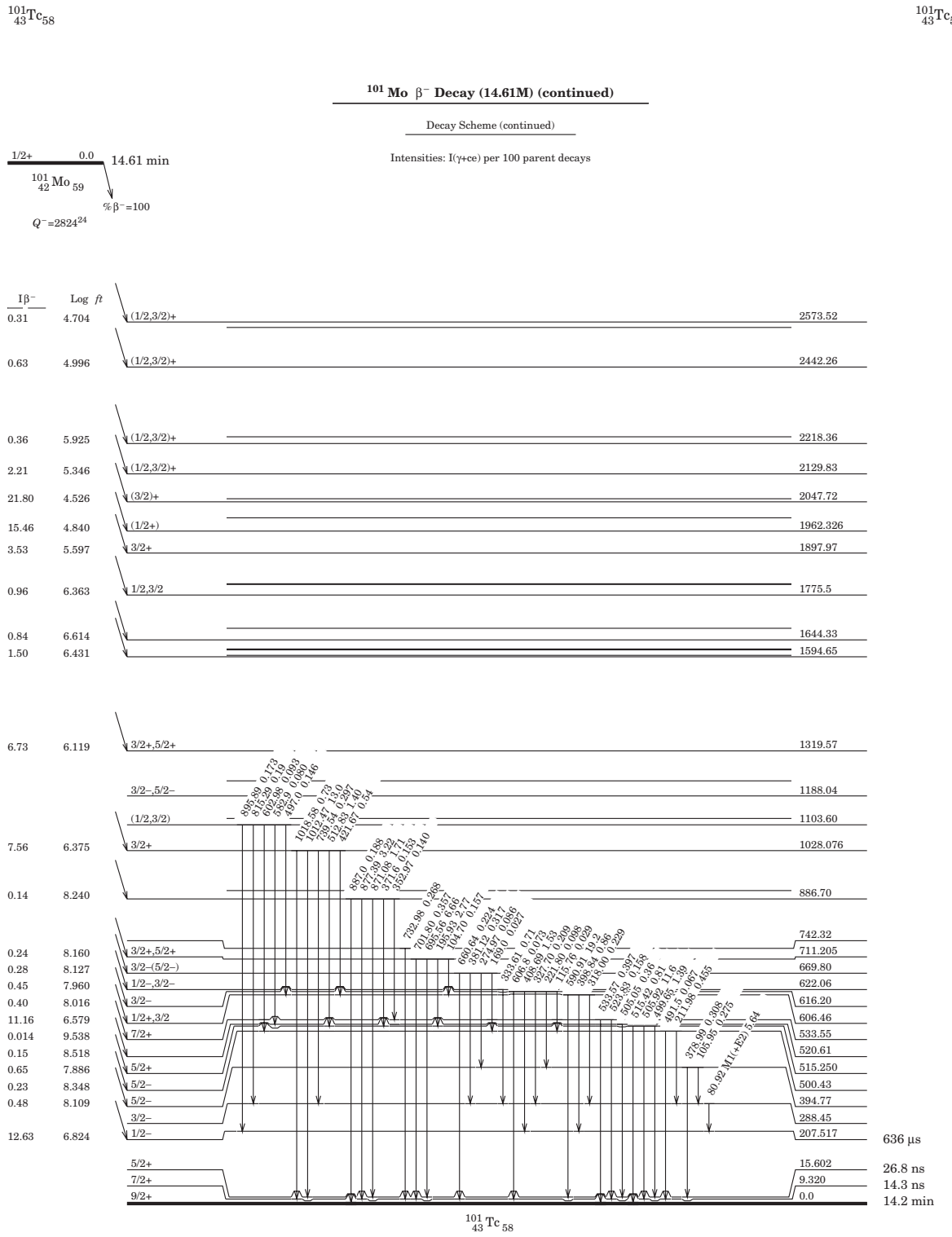

Fig. 2. *continued*

nucleus has a moderately-deformed prolate shape. Accordingly, in the following calculations, we thus construct the shell model basis at the deformation $\varepsilon_2 = 0.28$, and this is in accordance with that adopted in the work of Savage *et al.*,[3] in which a deformation of $\delta = 0.28$ is used in the symmetric particle-plus rotor model to interpret the structure observed in ^{101}Tc successfully, and from the comparison of Fig. 4 in ref. 3 and Fig. 10b in ref. 15, we have found that the deformation parameter δ used by Savage *et al.* is equal to ε used by Browne *et al.*,[15] and is also equal to ε_2 deduced from the Nilsson + BCS calculations in this work. The vacuum state $|\phi(\varepsilon_2 = 0.28)\rangle$ is hereafter written as $|0\rangle$. The hexadecapole deformation parameter $\varepsilon_4 = -0.007$ is taken from the compilation of Möller *et al.*[13]

Considering in the case of the positive-parity yrast band the odd-proton occupies a $1g_{9/2}$ orbital. So in the calculations, the basis states were restricted to the Nilsson states near the Fermi surface in the $N = 4$ major shell for protons,

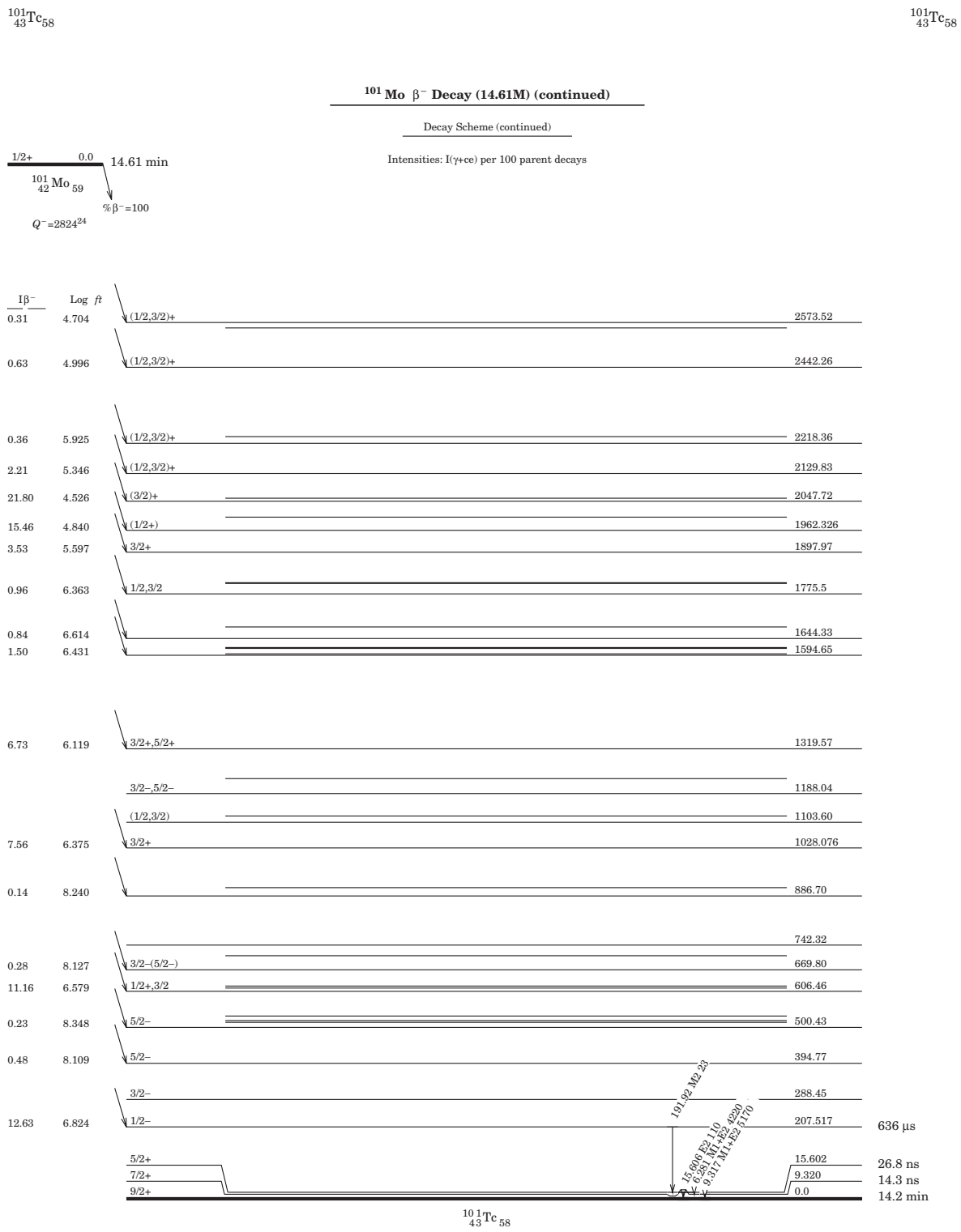

Fig. 2. *continued*

i.e., the $K = 1/2, 3/2, 5/2, 7/2$ orbitals of $g_{9/2}$ subshell for protons, whereas no states have been adopted for neutrons. The results of this calculation and the comparison with the experimental results are shown in Fig. 4. The experimental $5/2^+$, $7/2^+$, and $9/2^+$ levels have been taken from the compilation of Blachot,[6] the rest have been taken from the in-beam study of the nucleus ^{101}Tc by Hoellinger *et al.*[1] and Dejbakhsh *et al.*[2] In fact the $5/2^+$–$9/2^+$ levels have also been observed in the present work. It should be mentioned here that the theoretical calculation results cannot be compared with the experimental data directly. There should be a translation so that each theoretical band-head state is equal to the experimental one, and the same method is also used when the other bands are described in the framework of the PSM as presented below. As can be seen, the experimental data are described roughly well except for low-lying levels ($7/2^+$ and $9/2^+$). This calculation predicts a $7/2^+$ state as ground state for ^{101}Tc instead of a $9/2^+$ state,

Table II. The errors of the log *ft* values calculated by using the ENSDF analysis and checking program.

E (level)	Iβ^-	log *ft*	Error of log *ft*
2573.52	0.31	4.704	0.141
2557.97	0.89	4.330	0.133
2442.26	0.63	4.996	0.094
2237.87	0.73	5.568	0.063
2218.36	0.36	5.925	0.061
2129.83	2.21	5.346	0.054
2056.83	2.95	5.376	0.050
2047.72	21.80	4.526	0.049
2001.33	0.93	5.987	0.047
1962.326	15.46	4.840	0.045
1897.97	3.53	5.597	0.042
1808.50	0.60	6.515	0.039
1806.38	3.37	5.769	0.039
1775.5	0.96	6.363	0.038
1678.09	0.33	6.972	0.035
1644.33	0.84	6.614	0.034
1617.75	1.94	6.288	0.033
1614.83	1.93	6.294	0.033
1594.65	1.50	6.431	0.033
1319.57	6.73	6.119	0.027
1028.076	7.56	6.375	0.023
886.70	0.14	8.240	0.022
711.205	0.24	8.160	0.020
669.80	0.28	8.127	0.020
622.06	0.45	7.960	0.020
616.20	0.40	8.016	0.020
606.46	11.16	6.579	0.019
533.55	0.014	9.538	0.019
520.61	0.15	8.518	0.019
515.250	0.65	7.886	0.019
500.43	0.23	8.348	0.019
394.77	0.48	8.109	0.018
207.517	12.63	6.824	0.017

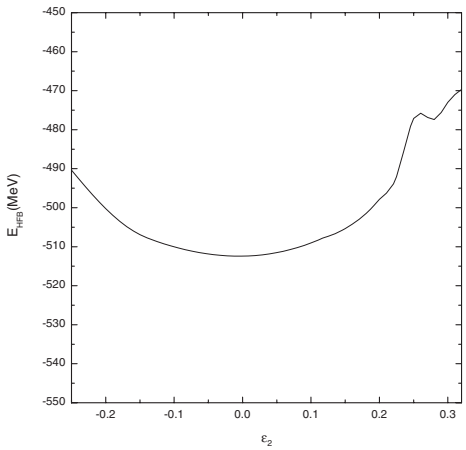

Fig. 3. Hartree–Fock–Bogoliubov energy E_{HFB} of ^{101}Tc as a function of quadrupole deformation parameter ε_2.

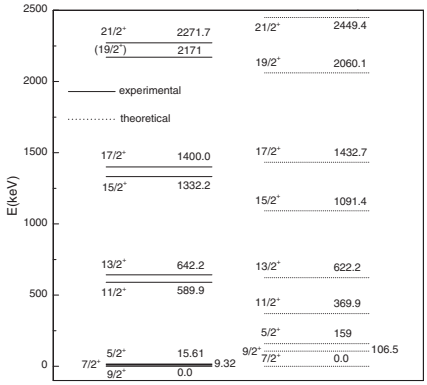

Fig. 4. Projected Shell Model calculations for positive-parity yrast states in ^{101}Tc compared with the experimental data.

just as the results from the Arias calculation within the IBFM-2 framwork.[16] The evolution of the yrast positive-parity states in Tc isotopes shows that, while ^{97}Tc exhibits the typical behaviour of the weak-coupling scheme, the excited states of heavier Tc isotopes evolve towards a strong-coupling scheme. This means that the proton Fermi level, which is close to the low-Ω states of the $\pi g_{9/2}$ subshell for the weakly-deformed ^{97}Tc nucleus, comes near the $5/2^+$ of the $\pi g_{9/2}$ subshell for $^{103-105}$Tc having a larger deformation. One can notice that ^{103}Tc is the first isotope to show the regular order of a rotational band even though the signature splitting remains very large.[17,18] The band associated with the $\pi g_{9/2}$ configuration shows a large signature splitting, which has been associated with a large γ deformation for some of the nuclei (e.g., Ag) in this region.[19] The calculated results also show this signature splitting, but not so large. This is maybe because our present computer code assumes axial symmetry, so that we cannot investigate those γ-deformed nuclei quantitatively.[20]

In fact in the present example of ^{101}Tc, where the positive-parity yrast band is originated from $\pi g_{9/2}$ configuration as mentioned above, one finds that the proton Fermi energy lies between the $K = 5/2$ and $K = 7/2$ qp states of the intruder $1g_{9/2}$ subshell. Therefore, orbitals around these levels are physically most important. To build a qp basis, the $K = 1/2, 3/2, 5/2$, and $7/2$ proton qp states of the intruder $1g_{9/2}$ subshell are selected. Whereas no neutron qp states are selected. Consequently, the dimension of our configuration space finally becomes 4. The shell model configuration space is constructed by projecting each of these qp states onto a good angular momentum and the Hamiltonian is diagonalized in this space. The band diagram as mentioned in ref. 14 is shown in Fig. 5. Filled circles in this figure represent the positive-parity yrast band numbers, which are obtained from the final diagonalization procedures (band mixing)[21] and also have been shown in Fig. 4. It is this kind of diagrams which one can conveniently use to extract physics out of the numerical results.[14] The lowest level ($I = 5/2$) has the nature of 1-qp band originated from $5/2^+[422]$ Nilsson state, indicating that the $K = 1/2$ and $K = 3/2$ states have little effect on this state, and the $K = 7/2$ band cannot participate in the calculation at this angular momentum because of the restriction $|K| \leq I$. Then the $K = 7/2$ band combine with the $K = 5/2$ band and makes contribution to this positive-parity yrast band. In short, the contribution will be great as they (also include $K = 1/2$ and $K = 3/2$ bands) approach the filled circles, that is, the positive-parity band.

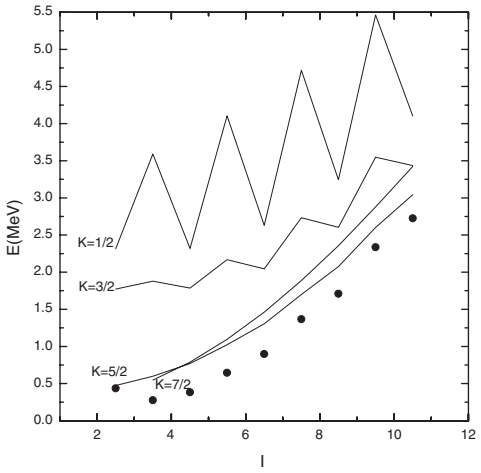

Fig. 5. A band diagram calculated for the positive-parity yrast band in ^{101}Tc (filled circles). All the results (filled circles included) are extracted from PSM calculations. Filled circles are the lowest states obtained after configuration mixing at each spin.

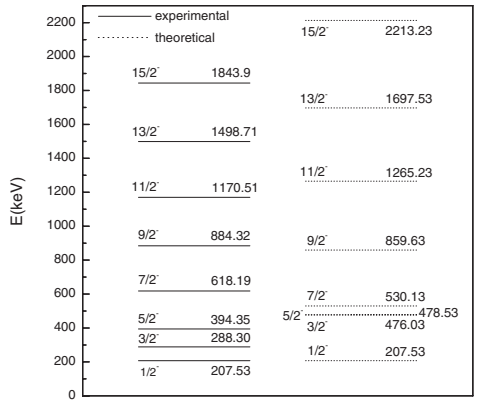

Fig. 6. The comparison of the experimentally observed negative-parity yrast band in ^{101}Tc with the predictions of the PSM.

In the negative-parity yrast band calculations, the configuration space is constructed by selecting the qp states close to the Fermi energy in the $N = 3$ major shell for protons, i.e., $\pi p_{1/2}$ orbital and other orbitals near it, whereas no qp states have been selected for neutrons. The negative-parity yrast band, calculated also for a $\varepsilon_2 = 0.28$ deformation parameter, seems to give the best reproduction of the experiment. The theoretical energy of the negative-parity yrast band is compared with the experimental data as shown in Fig. 6. The experimental levels have been taken from ref. 3. In fact the $1/2^-$–$5/2^-$ levels can also be found in the present measurement. This figure shows that the order of all calculated levels agrees with that of the experimental ones.

In Fig. 7 we showed the band members identified in ^{101}Tc originated from $3/2^-[301]$, $5/2^-[303]$, and $1/2^+[431]$ configurations adopted from ref. 3, respectively, and compared with the predictions of PSM, whereas the levels at 616.18, 669.28, 500.36, 606.41, 711.2, and 886.70 keV can also be specified in the present measurement. The $3/2^-[301]$ and $5/2^-[303]$ bands are reproduced roughly well. However, we found that the agreement with the $1/2^+[431]$ band was not satisfactory, the order of the calculated levels $1/2^+$ and $3/2^+$ disagreed with that of the experimental ones. But for these two states other spins are allowed experimentally both in the work of Savage *et al.*[3] and in our present work, and the particle-rotor model calculation associates this band with a relatively pure $1/2^+[431]$ Nilsson band, ranging from 58 to 91% depending on the spin.[3] Whereas in our PSM calculations of these three bands, the theoretical results are based on single basis, i.e., $3/2^-[301]$, $5/2^-[303]$, and $1/2^+[431]$ Nilsson states, respectively.[21] In other words, they are the results before the shell model diagonalization (band mixing).

5. Summary

In summary, the decay of ^{101}Mo has been reinvestigated using a γ–γ–t coincidence measurement. According to the off-line analysis, the positions of 7 γ-rays have been arranged again, particularly our placement of the 515.42 keV γ-ray transition differs from that reported previously.[4] 3 γ-rays have been placed in the decay scheme for the first time, the positions of 4 γ-rays have been reconfirmed, and one new γ-ray was observed and placed in the decay scheme. New results on β^- decay branching ratio, log *ft* value have been obtained. In addition, theoretical analysis of two low-lying bands designated as positive-parity yrast band that starts from $9/2^+$ and negative-parity yrast band that starts from $1/2^-$ is performed and compared with the

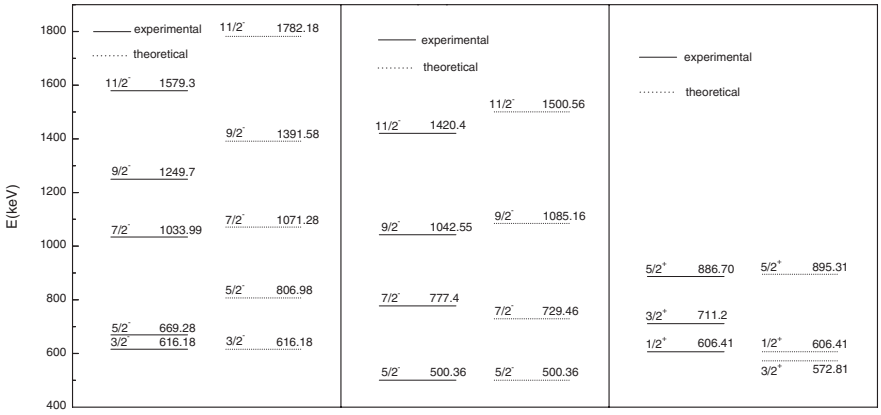

Fig. 7. Band members identified in ^{101}Tc originated from $3/2^-[301]$, $5/2^-[303]$, and $1/2^+[431]$ configurations adopted from ref. 3, respectively, and compared with the theoretical predictions of PSM.

experimental data, and other three pure rotational bands based on $3/2^-[301]$, $5/2^-[303]$, and $1/2^+[431]$ Nilsson states. In addition, a band diagram calculated for the positive-parity yrast band has been shown. The interpretation of the structure of ^{101}Tc in the framework of a PSM has proven to be successful.

Acknowledgements

We would like to thank the staff at Cyclotron in Shanghai Institute of Applied Physics, CAS. This Project is supported by the National Natural Science Foundation of China under Grant Nos. 10547140, 10405031 and 10475026. The authors are grateful to the Institute of Pure and Applied Physics for financial support in publication.

1) F. Hoellinger, N. Schulz, S. Courtin, B. J. P. Gall, M.-G. Porquet, I. Deloncle, A. Wilson, T. Kutsarova, A. Minkova, J. Duprat, H. Sergolle, C. Gautherin and R. Lucas: Eur. Phys. J. A **4** (1999) 319.
2) H. Dejbakhsh, G. Mouchaty and R. P. Schmitt: Phys. Rev. C **44** (1991) 119.
3) D. G. Savage, H. Aslan, B. Crowe, T. Dague, S. Zeghib, F. A. Rickey and P. C. Simms: Phys. Rev. C **55** (1997) 120.
4) M. A. Hammed, T. D. Mac Mahon and A. H. Naboulsi: Nucl. Instrum. Methods Phys. Res., Sect. A **334** (1993) 485.
5) J. F. Wright, W. L. Talbert, Jr., and A. F. Voigt: Phys. Rev. C **12** (1975) 572.
6) J. Blachot: Nuclear Data Sheets **83** (1998) 54.
7) S. Shen, Y. Li, S. Shi, J. Gu, J. Liu, K. Fang and J. Zhou: High Energy Phys. Nucl. Phys. **24** (2000) 306 [in Chinese].
8) B. Ding and N. Wang: Neutron Source Phys. (1984) 143 [in Chinese].
9) S. Shen, X. Yu, S. Shi, J. Gu, J. Liu, Y. Li and Z. Zhu: Eur. Phys. J. A **9** (2000) 463.
10) R. Palit, J. A. Sheikh, Y. Sun and H. C. Jain: Phys. Rev. C **67** (2003) 014321.
11) J.-Y. Zhang, N. Xu, D. B. Fossan, Y. Liang, R. Ma and E. S. Paul: Phys. Rev. C **39** (1989) 714.
12) A. Bohr and B. R. Mottelson: *Nuclear Structure* (Benjamin, New York, Amsterdam, 1969) Vol. I, p. 169.
13) P. Möller, J. R. Nix, W. D. Myers and W. J. Swiatecki: At. Data Nucl. Data Tables **59** (1995) 185.
14) K. Hara and Y. Sun: Int. J. Mod. Phys. E **4** (1995) 637.
15) *Table of Isotopes*, ed. C. M. Lederer and V. S. Shirley (John Wiley & Sons, New York, 1978) 7th ed., Appendix 38.
16) J. M. Arias, C. E. Alonso and M. Lozano: Nucl. Phys. A **466** (1987) 295.
17) A. Bauchet *et al.*: Acta Phys. Hung. N. S. **13** (2001) 189.
18) A. Bauchet *et al.*: Eur. Phys. J. A **10** (2001) 145.
19) H. J. Keller, S. Frauendorf, U. Hagemann, L. Kaubler, H. Prade and F. Stary: Nucl. Phys. A **444** (1985) 261; S. Frauendorf: Proc. Int. Symp. In-Beam Nuclear Spectroscopy, Debrecen, Hungary, 1984.
20) M. A. Rizzutto, E. W. Cybulska, L. G. R. Emediato, N. H. Medina, R. V. Ribas, K. Hara and C. L. Lima: Nucl. Phys. A **569** (1994) 547.
21) Y. Sun and K. Hara: Comput. Phys. Commun. **104** (1997) 245.